Bottom Simulating Reflector in the western Ross Sea (Antarctica)

Riccardo Geletti, Martina Busetti

Riccardo Geletti (rgeletti@inogs.it)

Martina Busetti (mbusetti@inogs.it)

Present affiliation and postal address for all authors:

National Institute of Oceanography and Applied Geophysics - OGS

Borgo Grotta Gigante 42/c, 34010 Sgonico (Trieste), Italy

Cite this chapter:

Geletti, R., Busetti, M. (2022). Bottom Simulating Reflector in the Western Ross Sea, Antarctica. In: Mienert, J., Berndt, C., Tréhu, A.M., Camerlenghi, A., Liu, CS. (eds) World Atlas of Submarine Gas Hydrates in Continental Margins. Springer, Cham. https://doi.org/10.1007/978-3-030-81186-0_40

Abstract Seismic evidence of the presence of gas hydrates and free gas in the western Ross Sea (Antarctica), is inferred from the occurrence of a Bottom Simulating Reflector (BSR). The BSR, from the deeper basin to an intra-basin structural high, evolves into Cross-Cutting Reflectors (CCRs) and Enhanced-Amplitude Reflectors (EARs). The presence of free gas, is deduced, besides the seismic data analysis, also by the occurrence of gas seeping seafloor morphologies like mud volcanoes and pockmarks. The upward gas migration, connecting the free gas zone below the BSR and the mud volcanoes and pockmarks on the seafloor is controlled by the presence of faults.

1.1 Introduction

The continental margin of the Ross Sea has been extensively surveyed since late ’80, but only in a limited area located in the western side, evidence of Bottom Simulating Reflector (BSR), inferred to reveal the base of a zone of gas hydrate, have been found (Geletti and Busetti, 2011). Contrary to the first discoveries that took place in Antarctica, where the BSR was found as a clear continuous reflector on the continental rise of the Wilkes Land and Antarctic Peninsula

(Kvenvolden et al., 1987; Lodolo et al., 1993), that of the Ross Sea are on the continental shelf and appears more complex (Geletti and Busetti, 2011), preventing immediate identification. After detailed reprocessing to preserve the true amplitude and the shape of the wavelet, the multichannel seismic data analysis clearly reveals different type of high amplitude cross cutting reflectors, including a strong BSR related to the occurrence of gas hydrate/free gas (Geletti and Busetti, 2011). Seabed morphological features as mud volcanoes and pockmarks confirm that the system is characterized by the presence of fluids/gas, which migrate towards the surface through the gas chimneys set on faults.

1.2 Regional setting of western Ross Sea

The Ross Sea is a major embayment in the Antarctic coastline, about 1000 x 1000 km large, located on the wide continental shelf with an average water depth of about 500 m. The Cenozoic rift phase produced four main basins where several kilometers of Cenozoic fluvial/continental to marine deposits, and with occurrence of diamicton (very poorly sorted sediment deposited by glaciers in moraines) since the Miocene period (Brancolini et al., 1995).

The N-S elongated Victoria Land basin, one of the four tectonic basins about 150 km wide and 400 km long, is located in the south-western Ross Sea (Fig. 1.1), and represents the deepest basin in the Ross Sea filled by more than 10 km of sediments (Cooper et al., 1987; Brancolini et al., 1995). Since Oligocene, the Victoria Land Basin has been affected by a renewed phase of tectonic activity and magmatic intrusions, generating the Terror Rift constituted by the Lee Arch running north-south from the Melbourne to the Erebus active volcanoes, and by the depocenter of the Discovery graben (Cooper et al., 1987; Sauli et al., accepted). Presently, the sea floor depth of the Discovery graben is more than 1000 m, exceeding 1500 m in front of the Drygalski Ice Tongue.

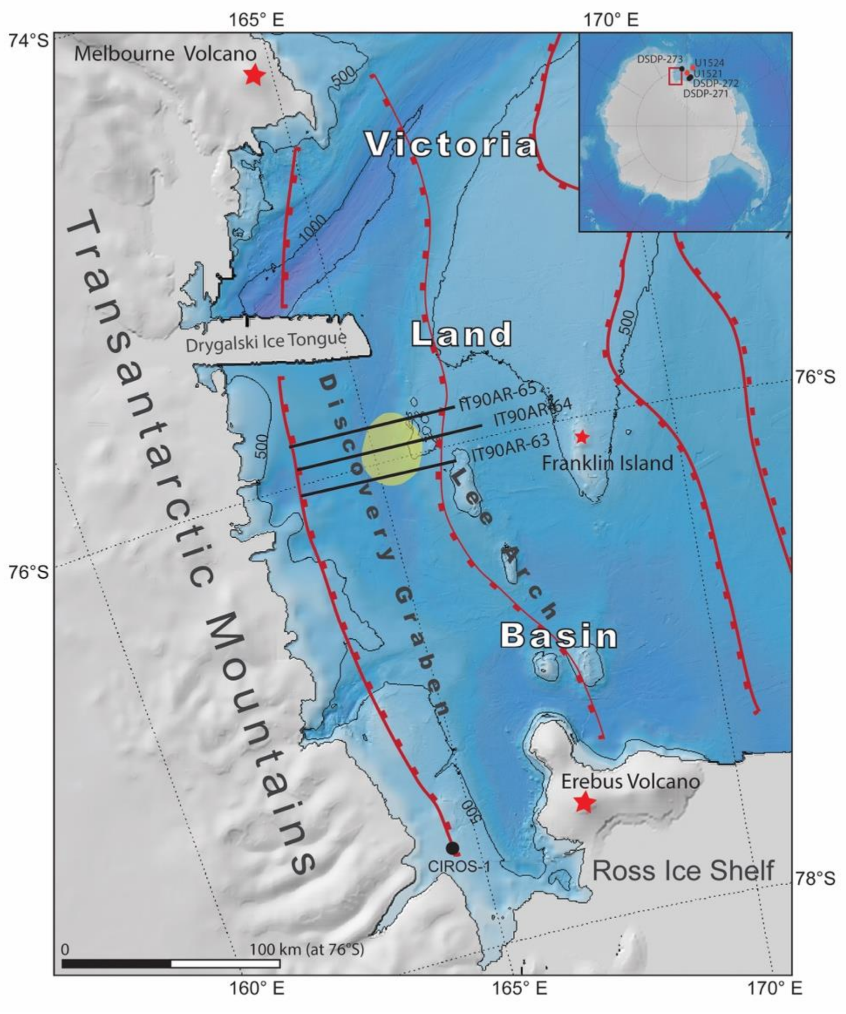

Fig. 1.1 - The map of Western Ross Sea with the position of the studied multichannel seismic profiles and the area (yellow) with the occurrence of the Bottom Simulating Reflectors (BSRs), Cross Cutting Reflectors (CCRs) and Enhanced-Amplitude Reflectors (EARs) as base of gas hydrate. The DEM model is made with GeoMapApp (www.geomapapp.org; CC by Ryan et al. 2009), red stars indicate recent volcanoes, red lines are the borders of the sedimentary basins.

In the Ross Sea the concentration of gas (mainly methane and minor ethane) is low in the shallow sediment sampled by gravity core (Rapp et al., 1987), or by DSDP (McIver, 1975) and

IODP drilling (McKay et al., 2019). The gas concentration increases in deeper Miocene muddy sediments (64-365 mbsf) recovered from DSDP sites 271, 272 and 273, in the eastern and north-western part of the Ross Sea, with contents of total hydrocarbon gas (mainly methane), up to 179,000 ppm in the DSDP 273 (McIver, 1975), that isotopic analysis with very negative $\delta^{13}C$ values, suggests that they are more likely to be of shallow biogenic origin (Claypool and Kvenvolden, 1983), and in the IODP sites U1521 and U1524 in the eastern Ross Sea with content of 67,000 ppmv methane and 264 ppmv ethane and 42,000 ppmv of methane respectively (McKay et al., 2019). At CIROS-1 well, the Oligocene to Miocene rocks contain small amount of organic carbon, (Collen et al., 1989), with a thin level of Late Eocene sandstone (632-634 m) containing an asphaltic residue, which has been suggested to be the residue from a migrated hydrocarbon (Cook and Woolhouse, 1989). Considering the increase of gas concentration in the deepest sediment, both McIver [1975] and Rapp et al. [1987] speculated that the gases may have been immobilized as gas hydrates, but at that time, evidence of clathrates or BSRs in seismic profiles was not observed.

The theoretical occurrence of the Gas Hydrate Stability Zone (GHSZ) was modelled locally in central Victoria Land basin by Geletti and Busetti (2011) and regionally for the Ross Sea by Giustiniani et al., (2018). Geletti and Busetti (2011) using Sloan equation (Sloan, 1990) for methane, assuming that in the seismic profile IT90AR-63S the GHSZ is at depth of 350 m mbsf and the depth of the Gas Hydrate Equilibrium Zone is at 600 m bsl, estimated that the average geothermal gradient is 36°C/km. This value is consistent with those calculated from hundred-meter-deep wells in southern VLB ranges from 24 to 40 °C/km (Geletti and Busetti, 2011 and reference therein). Giustiniani et al., (2018), evaluated the theoretical GHSZ in the Ross Sea by mean of a steady state simple modeling on the base of bathymetric data, sea bottom temperature, heat flow, assuming that the natural gas is methane, and considering two end member variable geothermal gradient of 49°C/km and 103°C/km. For the same site of Geletti and Busetti (2011), their results suggest that the GHSZ is at 310 m bsl and at 130 m bsf for the average geothermal gradient of 49°C/km and of 103°C/km, respectively. Both models are quite consistent for the lower geothermal gradient, considering that the geothermal gradient is a variable poorly constrain in the study area.

1.3 BSR Types and Distribution

Reprocessing the multichannel seismic data (3000 m streamer, 120 channels, 60 fold), using the software packages Focus™ and GeoDepth® by Paradigm™, highlighted the occurrence, within the Oligocene/Miocene sediment, of three types of high-amplitude reflectors, with negative or positive polarity and low frequency events, associated with velocity anomalies (Fig. 1.2):

- The Bottom Simulating Reflector, characterized by very high amplitudes, a phase inversion relative to the seafloor reflection event, and a tendency to parallel the seafloor topography, while crosscutting the local seismic stratigraphy (Fig.s 1.2 - 1.6). Above the BSR, the interval velocities are about 1900-2050 m/s and below it they drop to about 1360 to 1400 m/s. The dominant frequency of the BSR is about 20 Hz, lower than the 25 Hz of the stratigraphic reflectors occurring at the same time window (Fig. 1.5c). The BSR is more continuous in the eastern side of the Discovery Graben, where is also cut by faults (Fig. 1.2, 1.5, 1.6).
- Cross Cutting Reflectors (CCRs) have the same seismic characteristics of the BSR, but they do not mimic the seafloor. CCRs are present in the western side of the Lee Arch only in the southernmost profiles (Fig.s 1.2b,c, 1.5), rising up from 300 to 150 ms in correspondence

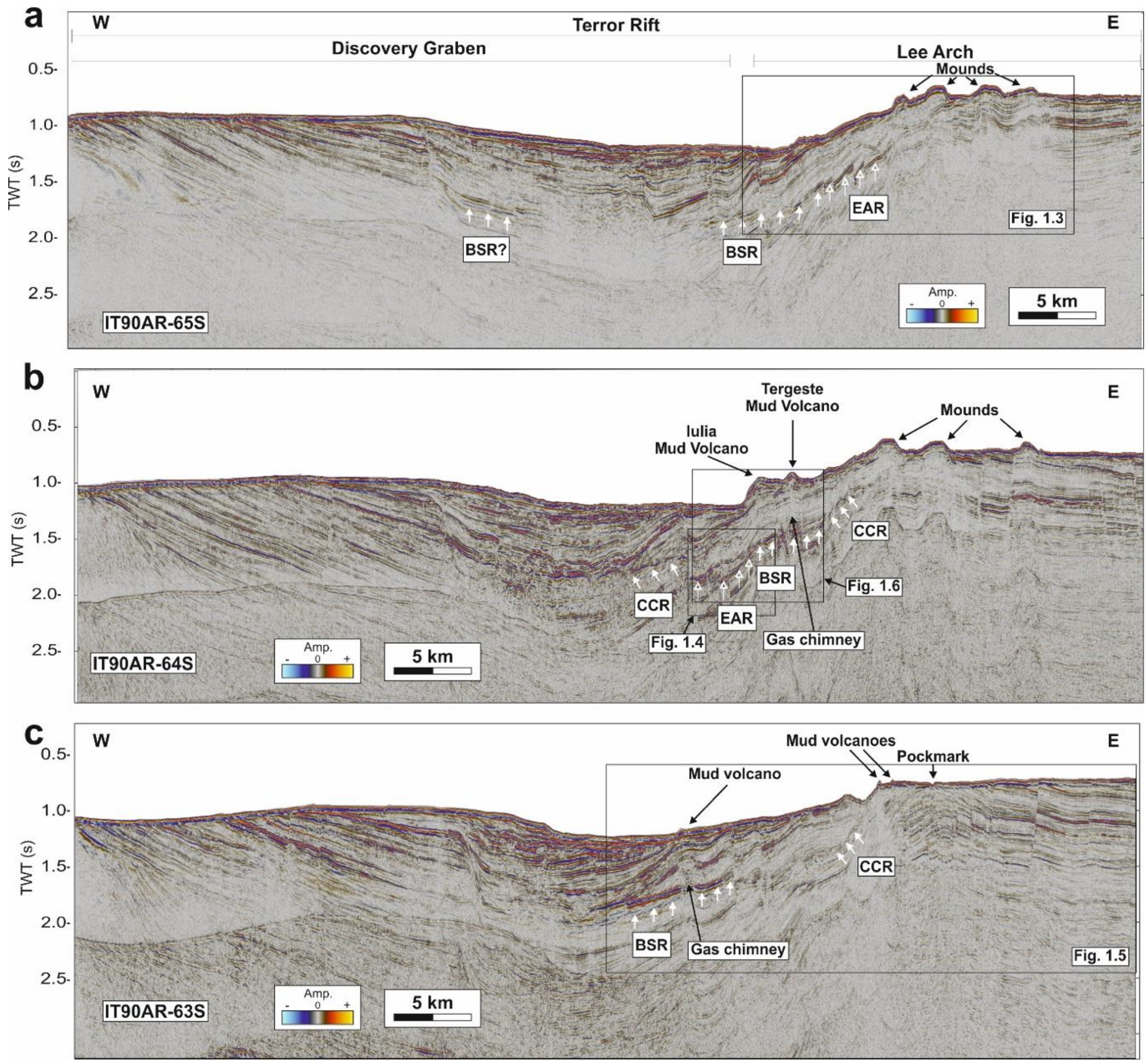

Fig. 1.2 - Migrated multichannel seismic profiles (a) IT90AR-65S, (b) -64S and (c) -63S, collected by OGS in 1990 showing the Bottom-Simulating Reflector (BSR), Cross-Cutting Reflectors (CCRs) and Enhanced-Amplitude Reflectors (EARs). The seafloor morphology is characterized by mud volcanoes and pockmarks and mounds.

with a 1.5 km wide depression in the seafloor. Above the CCRs the interval velocities are about 2000 m/s and they drop to about 1400 m/s below (Fig. 1.5). The CCRs, occurring in the area of active faults, could not be identified as a proper BSR, because of the reflectors depth offsets between each fault segment. As suggested by Vanneste et al. (2003) these offsets can be caused by fluid convection cells which disturb the local gas-hydrate stability conditions.

- Enhanced Amplitude Reflections *(EARs)* are coherent seismic reflections, characterized by high amplitude, reverse polarity and low frequency. They are present in the Lee Arch (Fig.s 1.2a,b, 1.3, 1.4, 1.6). The dominant frequency is about 22 Hz. Occasionally, the EARs are identified by a borderline top termination against the BSR (Fig. 1.3). The EARs are seismo-stratigraphic reflectors related to sediments that likely have higher porosity than the surrounding media, providing a preferential zone for the free gas accumulation (Judd and Hovland, 2007). Similar to the stratigraphy, the EARs could be faulted and tilted, as occurs along the profile IT90A-65 (Fig.s 1.2a, 1.3). The top terminations follow the Base of the Gas Hydrate Stability Zone (BHSZ), as reported in the Norwegian margin by Berndt et al. (2004). The bottom terminations of the EARs, with changing amplitude, frequency and phase, follow a trend deeper and sub-parallel with the BGHSZ (Fig.s 1.2a, 1.3). An alternate possibility could be that the bottom terminations are determined by how much gas migrates into each reflector.

Moving from the basin to the Lee Arch, the BSR transitions to CCRs and EARs. This behavior can be related to transitions in the sediment characteristics, geothermal gradient, and flow behaviors of fluid and gas. Broadly speaking, the BSR is present in the less active zone, where pressure, temperature and flow characteristics are laterally homogeneous. On the other hand, the CCRs and EARs are present in the most faulted area, where strands separate the area into blocks, each with a distinct geothermal gradient, flow characteristics and gas availability. The overall distribution of the BSR, CCRs and EARs, covers an area of approximately 600 km^2 (Fig. 1.1).

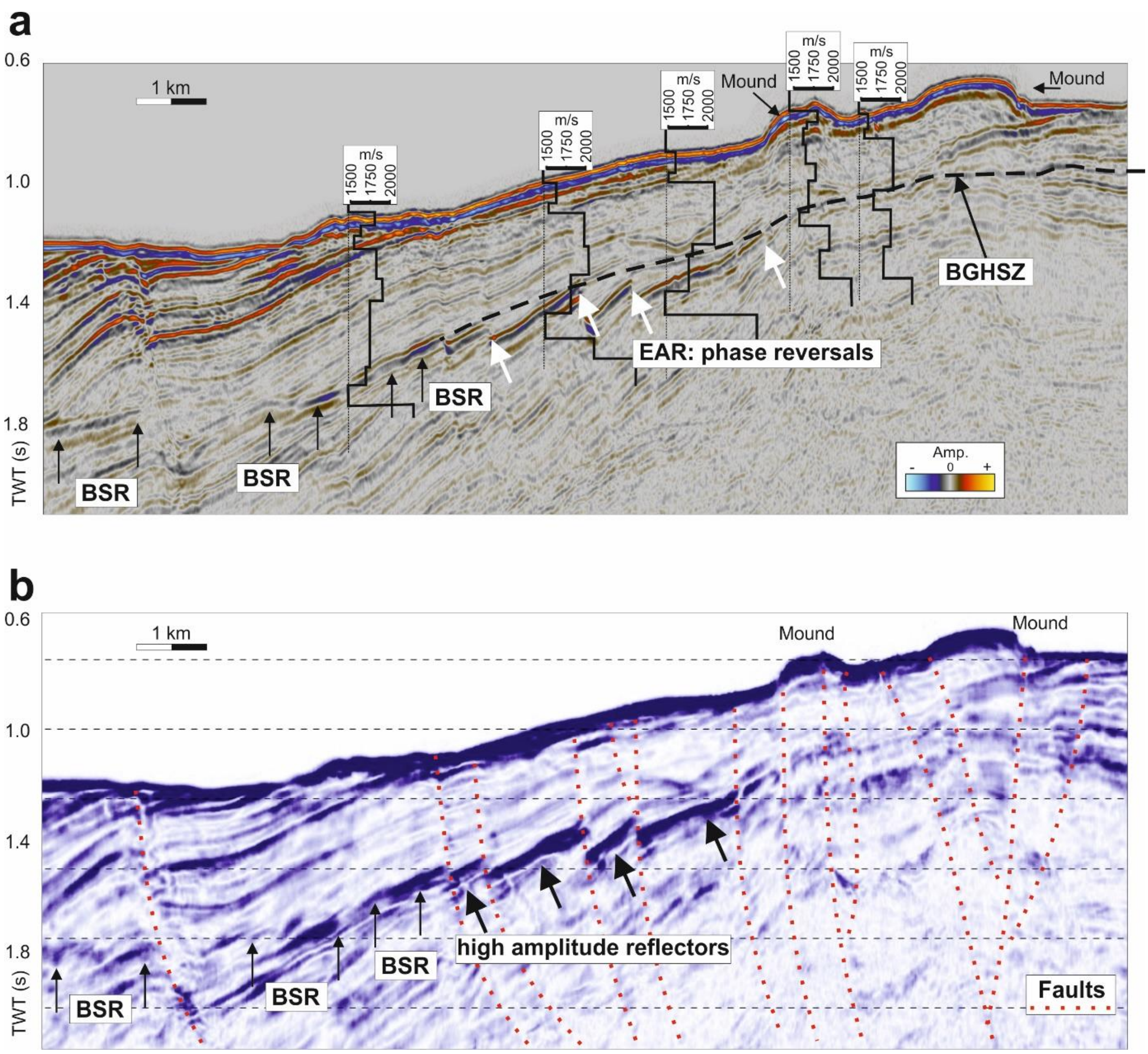

Fig. 1.3 - Migrated seismic section IT90AR-65S (a) with velocity functions, and the relative reflection strength section (b) (see Fig. 1.1 for location) (modified after Geletti and Busetti, 2011). The Enhanced-Amplitude Reflections (EARs), disrupted by faults, show phase inversion in (a) and high reflection strength in (b) and the velocity drop to about 1350 m/s, provides evidence of a free-gas zone. The dashed line in (a) is the borderline top of EARs termination that shows a bottom simulating trend, and is the continuation of the BSR and the BGHSZ.

Hence, the stability field of gas hydrates varies from section to section, segmenting the BSR into CCRs and EARs. Complex seismic trace attributes, reflection strength (also known as instantaneous amplitude or envelope amplitude) and instantaneous frequency (Taner and Sheriff, 1977), were extracted to highlight the free-gas occurrence (Fig.s 1.3, 1.5, 1.6). The reflection strength depends on the contrast of seismic impedance (i.e. velocity times density) and it is independent of the effects of phase distortion in the stacked seismic section.

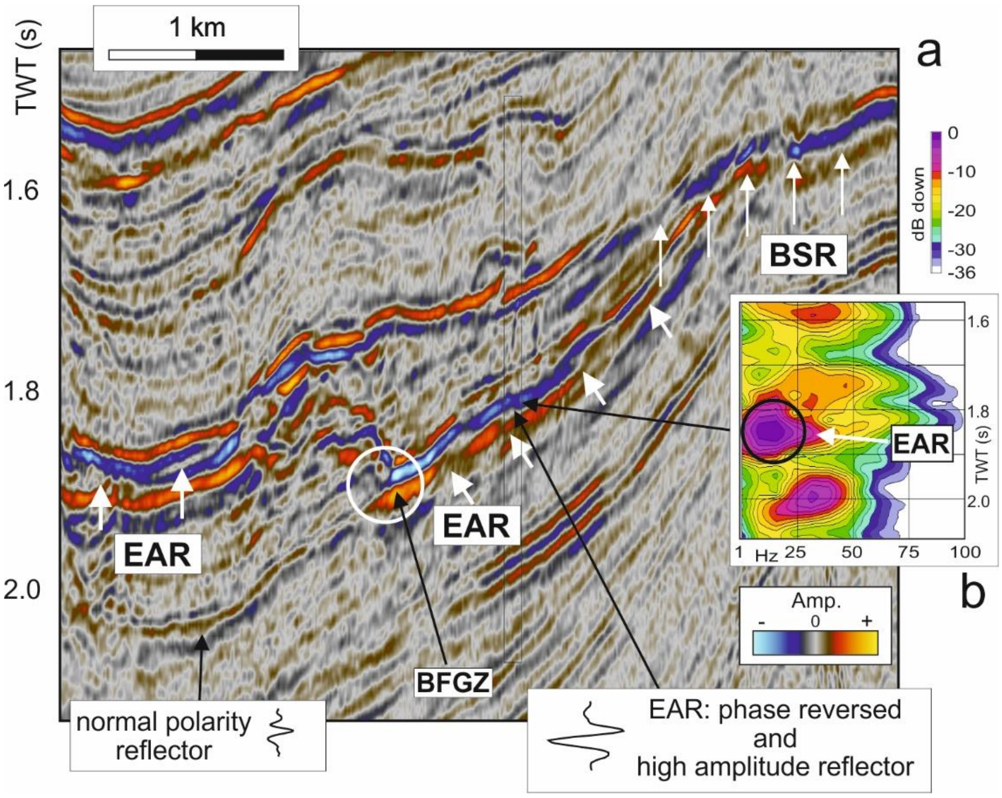

Fig. 1.4 - BSR and Enhanced Amplitude Reflection (EAR) (see Fig. 1.2 for location), under the mud volcano system (a). The EAR shows high amplitude reverse polarity and low frequency (black circle in b where it shows the frequency spectrum vs TWT panel) that are related to the occurrence of free gas above it. The event in the white circle (a) shows the change of polarity that corresponds to the Base of Free Gas Zone (BFGZ) under the BSR.

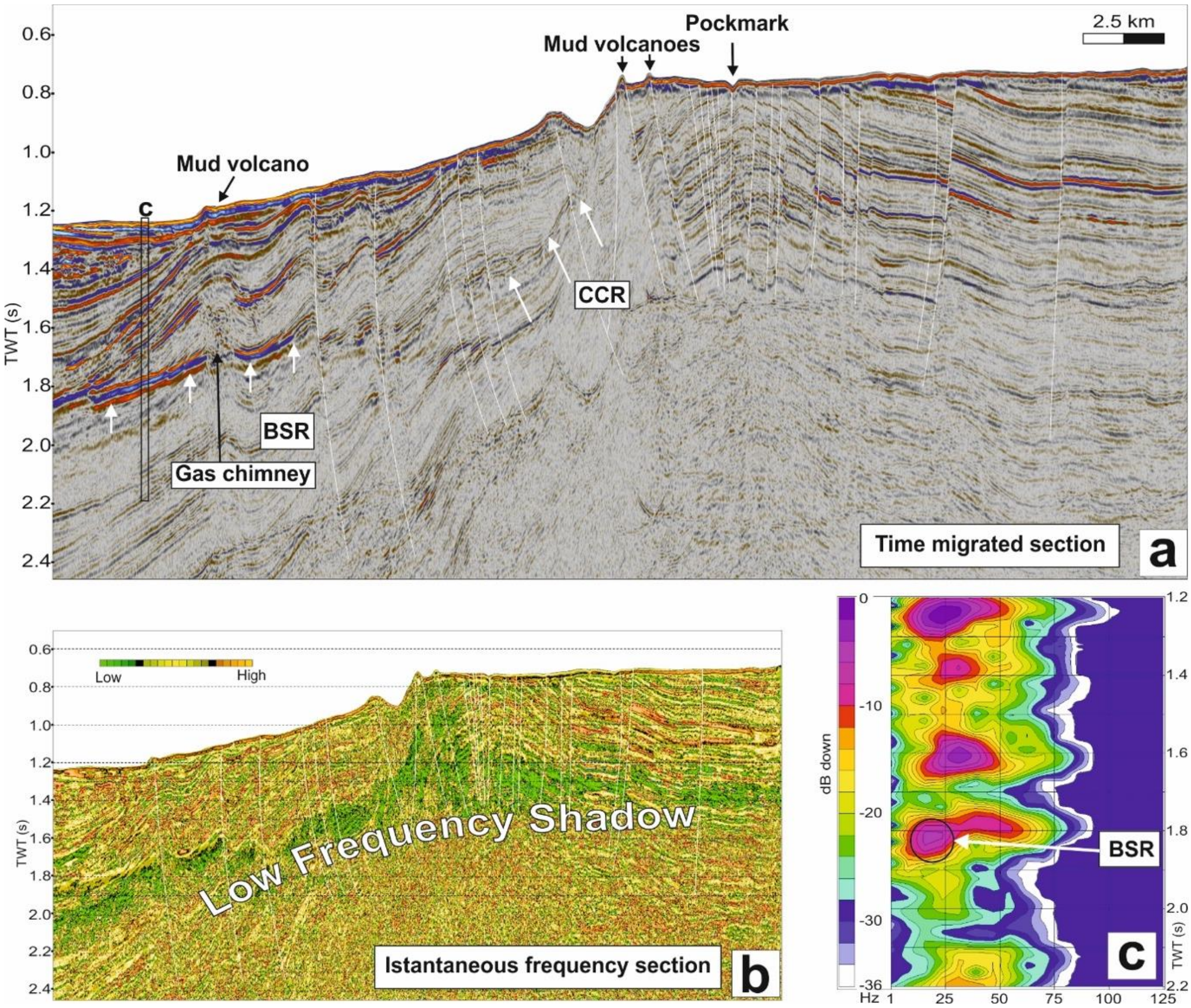

Fig. 1.5 - Stack with true-amplitude approach (a) and instantaneous frequency section (b) of IT90A-63S (see Fig.1.2 for location) (modified after Geletti and Busetti, 2011). In a) the BSR, Cross-Cutting Reflectors (CCRs) and Enhanced-Amplitude Reflectors (EARs) are present. In the instantaneous frequency section a wide and almost continuous area characterized by low frequencies shadow (green colour), follows the distribution of the BSR, the CCRs EARs. The low frequency (in black circle in c - the frequency spectrum vs TWT panel) is an indicator of the free-gas occurrence.

Hence, a high-reflection strength is often associated with gas accumulations (Taner et al., 1979). According to the principle that gas occurrence attenuates high frequencies (Taner et al., 1979; Carcione and Picotti, 2006), the data were displayed as an instantaneous frequency section that produces a “low frequency shadow” over the region of inferred free gas (Fig. 1.5b) (Taylor et al., 2000, Vanneste et al., 2002). The “low frequency shadow” follows the distribution of the BSR, CCR and EARs, with the low frequencies, between 5-20 Hz, related to the free-gas presence appear at shallow depth locations beneath the Lee Arch (Fig. 1.5b).

The geophysical characters of the BSR (reverse polarity and drop of velocities), indicate the relationship with gas occurrence rather than to the diagenesis of siliceous sediments BSR. The diagenesis related BSR results from the positive acoustic impedance contrast between two forms of opal of dissimilar density (increasing with depth). Hence, diagenesis related BSR shows a positive polarity as the seafloor reflection event (Hein et al., 1978; Davies and Cartwright, 2002), in contrast to the negative polarity associated with the hydrate-related BSR. A second difference between hydrate and diagenetic based BSRs is their response to seawater depth. With increasing water depth, the diagenesis related BSR has a constant depth below the seafloor or even decreasing subbottom depth due to the opal transition pressures occurring at shallower depths (e.g., Bohrmann et al., 1994), while the hydrate related BSR is parallel the seafloor topography.

In some cases the lateral variations in amplitude of the BSR are linked to tectonic characteristics (Pecher et al. 1998). Bouriak et al. (2000) have suggested that such variations are caused by percolation of the fluid upwards, where impermeable horizons or gas hydrates control the flow of fluids. Rowe and Gettrust (1993) reported vertical offsets in the BSR on Blake Ridge that were clearly associated with faults. Since the BSR is expected to adapt to local thermodynamic conditions, the persistence of these offsets suggests that faulting has altered the geothermal field, altering fluid circulation. In addition, magmatic intrusions present along the Lee Arch may leads to a localized increase in the geothermal gradient, thus causing a local rise towards the sea floor surface of the BSR.

The discontinuity of BSR may be caused by the lack of seismic evidence of the free gas, if e.g. there is not enough pore space or saturation is too low, that may be caused by sediment overcompaction and/or fluid expulsion due to glacial loading. The amplitude of the seismic signal (acoustic impedance contrast) depends of the reservoir properties, such as, dry-rock moduli, porosity, permeability and fluid properties, and in situ conditions such as pore pressure and temperature. The pore pressure as a function of depth depends on many factors, most of them of geological nature, such as low-permeability regions, sealing faults and hydrocarbons caps, which prevent pressure equilibration from the reservoir to the surface. (e.g., Carcione and Tinivella, 2001; Gei and Carcione, 2003; Carcione et al., 2006).

1.3.1 Mud volcanoes and pockmark formed by fluid/gas migration

Further evidence of gas occurrence is the presence of mud volcanoes and pockmarks, which are necessarily fed by fluids/gas. The gas comes mainly from the free-gas-bearing sediment between the BSR and the BFGZ. The gas hydrate acts as a trap for the underlying gas, but along fractures/faults the gas can migrate through the shallow sediment up to the seafloor, forming gas seeps associated with mud volcanoes and pockmarks (Fig.s 1.2, 1.6). The mud-volcanoes are fed by chimneys characterized by low seismic amplitude along the conduit, cutting across the stratigraphy down to the BSR suggests a gas/fluid and fluidized sediment upward migration (Fig.s 1.2, 1.4, 1.6).

The two main mud volcanoes, named Iulia and Tergeste, 2500 m x 1500 m wide and 80 m high, and 2000 m x 750 m wide and 40 m high, respectively, are located atop strands belonging to the fault system of the Lee Arch, and their elongated morphology develops following the N-S direction of the faults (Fig.s 1.2b, 1.6).

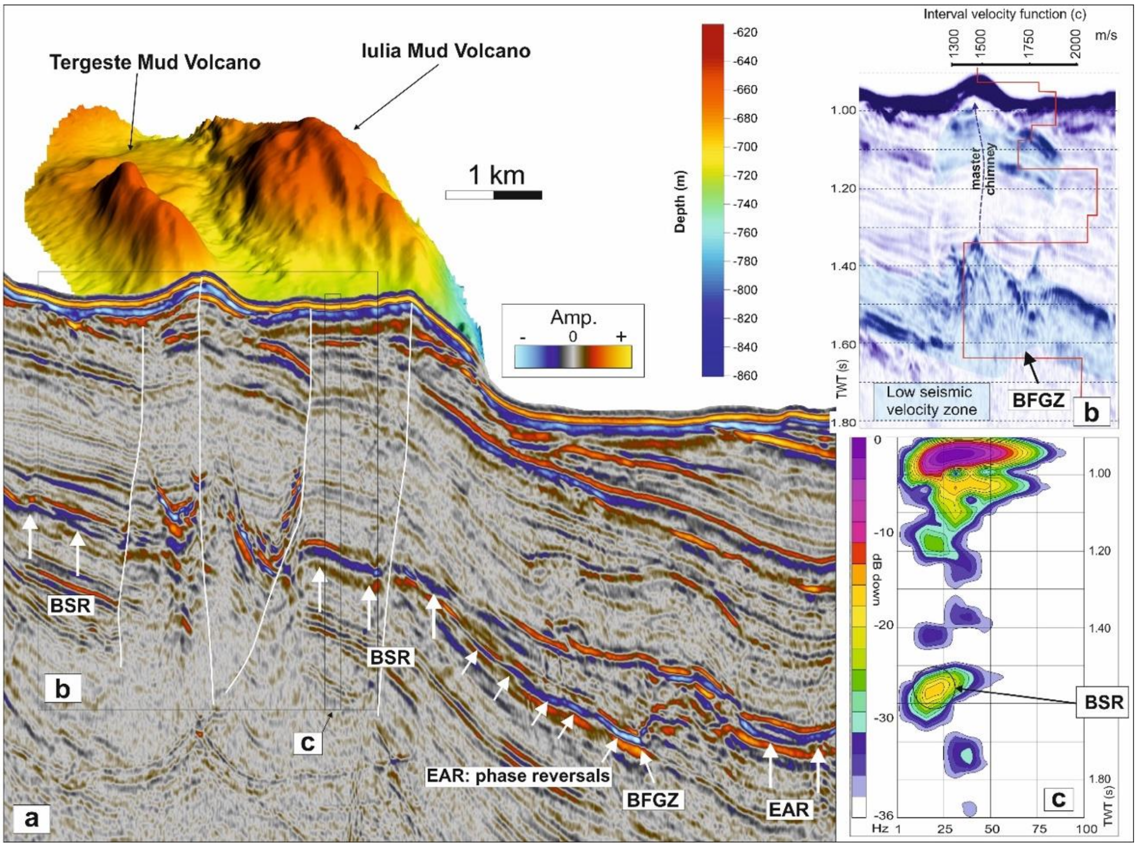

Fig. 1.6 - Seismic-migrated section IT90AR-64S (see location in Fig. 1.2b) and swath bathymetry across the Tergeste and Iulia Mud Volcanoes (a) with the BSR, EAR and the Base of Free Gas Zone (BFGZ) (modified after Geletti and Busetti, 2011), (b) relative reflection strength section with the interval velocity profile showing low velocity zone related to gas/fluid occurrence, and (c) frequency spectrum vs TWT panel with the dominant 20 Hz of the BSR respect the 24 Hz of the stratigraphy at the same depth.

Seabed topflat mounds, up to 4 km wide and 100 m high, occur on the Lee Arch. Although initially they were considered magmatic bodies (Cooper et al., 1987; Lawver et al., 2012), their origin is still not clear. They can be like mud carbonatic mounds, originated by hydrocarbon seepage favoring the pioneer chemosynthetic ecosystem on which successively the corals grow.

1.5 Summary

Evidence of the presence of gas hydrates and free gas in Victoria Land Basin (western Ross Sea, Antarctica) is inferred from the analysis through targeted reprocessing of the multichannel seismic reflection data, that have revealed the evidences of Bottom Simulating Reflectors (BSRs), Cross Cutting Reflectors (CCRs) and Enhanced-Amplitude Reflectors (EARs) as base of gas hydrate. The distribution of the low frequencies of the seismic reflections, indicating free-gas occurrence, forms a “low frequency shadow” that follows the transitions from BSR to CCRs and then to EARs.

The occurrence of free gas in the sediment is also revealed by the presence of mud volcanoes and pockmarks, which are necessarily feed by fluids/gas seeping, migrating upwards along chimneys mainly tectonically controlled.

Acknowledgments

The Authors thank the Programma Nazionale di Ricerche in Antartide - PNRA (*Italian Antarctic National Program*) for supporting the acquisition of the data multichannel seismic and the swath bathymetric data in 1990 and 2006 respectively, conducted by OGS by using the R/V OGS Explora, and for the PNRA-RIMARS and PNRA-VALFLU projects among which the authors analyzed the seismic profiles.

References

Berndt, C., S. Bünz, T. Clayton, J. Mienert, and M. Saunders, 2004, Seismic character of bottom simulating reflectors: examples from the mid-Norwegian margin. Marine and Petroleum Geology, v. 21(6), p. 723-733.

Brancolini, G., M. Busetti, A. Marchetti, L. De Santis, C. De Cillia, C. Zanolla, F. Coren, A. K. Cooper, G. Cochrane, I. Zayatz, V. Belyaev, M. Knyazev, O. Vinnikovskaya, F. Davey, and K. Hinz, 1995, Seismic Stratigraphic Atlas of the Ross Sea, Antarctica. In Geology and seismic stratigraphy of the Antarctic Margin, Antarctic Research Series, v. 68, edited by A. K. Cooper, P. F. Barker, and G. Brancolini, 22 Plates, AGU, Washington, D.C.

Bohrmann, G., A. Abelmann, R. Gersonde, H. Hubberton, and G. Kuhn, 1994, Pure siliceous ooze, a diagenetic environment for early chert formation. Geology, v. 22(3), p. 207-210.

Bouriak S., Vanneste M., Saoutkine A., 2000, Inferred gas hydrates and clay diapers near the Storegga Slide on the southern edge of the Voring Plateau, Offshore Norway. Marine Geology, 163, 125-148.

Carcione, J. M., and S. Picotti, 2006, P-wave seismic attenuation by slow-wave diffusion: Effects of inhomogeneous rock properties. Geophysics, v. 71(3), O1-O8, doi:10.1190/1.2194512.

Carcione, J.M., Picotti, S., Gei, D., Rossi, G., 2006, Physics and seismic modeling for monitoring CO2 storage. Pure and Applied Geophysics, 163(1), pp. 175-207.

Carcione, J.M. and Tinivella, U., 2001, The seismic response to overpressure: A modeling methodology based on laboratory, well and seismic data. Geophysical Prospecting, 49, 523–539.

Claypool, G., and K. Kvenvolden, 1983, Methane and other hydrocarbon gases in marine sediment. Annual Review of Earth and Planetary Sciences, v. 11, p. 299-327.

Collen J. D., Y. Xinghua, R. J. Collier, and J. H. Johnston, 1989, Hydrocarbon source rock potential and organic maturation, in Antarctic Cenozoic history from the CIROS-1 drillhole, McMurdo Sound. DSIR Bullettin 245, edited by Barrett P. J., pp. 223-230, DSIR Publishing, Wellington.

Cook, R.W., and A.D. Woolhouse, 1989, Hydrocarbon residue. In: Barrett, P. (ed.), Antarctic Cenozoic history from the CIROS-1 drillhole, McMurdo Sound. DSIR Bulletin, v. 245, p. 211-217.

Cooper, A. K., F. J. Davey, and J. C. Behrendt, 1987, Seismic stratigraphy and structure of the Victoria Land Basin, Western Ross Sea, Antarctica. In: The Antarctic Continental Margin: Geology and Geophysics of the Western Ross Sea. CPCEMR, Earth Science Series, v. 5B, edited by A. K. Cooper and F. J. Davey, p. 27-76, Huston, Texas.

Gei, D., Carcione, J.M., 2003, Acoustic properties of sediments saturated with gas hydrate, free gas and water. Geophysical Prospecting, 51(2), pp. 141-158.

Geletti, R., and M. Busetti, 2011, A double bottom simulating reflector in the western Ross Sea, Antarctica. Journal of Geophysical Research: Solid Earth, v. 116, B04101, doi.org/10.1029/2010JB007864.

Giustiniani M., U. Tinivella, C. Sauli, and B. Della Vedova, 2018, Distribution of the gas hydrate stability zone in the Ross Sea. Antarctica. Andean Geology, v. 45(1), p. 78-86.2018 doi: 10.5027/andgeoV45n1-2989

Judd, A. and M. Hovland, 2007, Seabed Fluid Flow. The Impact on Geology, Biology and the Marine Environment, Cambridge University Press, pp. 492.

Kvenvolden, K. A., M. Golan-Bac, and J. B. Rapp, 1987, Hydrocarbon geochemistry of sediments offshore from Antarctica: Wilkes Land continental margin. In: The Antarctic Continental Margin: Geology and Geophysics of Offshore Wilkes Land. CPCEMR, Earth Science Series, vol. 5A, edited by S. L. Eittreim and M. A. Hampton, pp. 205-213, Huston, Texas.

Lawver L., J. Lee, Y. Kim, and F. Davey, 2012, Flat-topped mounds in western Ross Sea: Carbonate mounds or subglacial volcanic features? Geosphere; v. 8(3), p. 645–653; doi:10.1130/GES00766.1

Lodolo, E., A. Camerlenghi, and G. Brancolini, 1993, A bottom simulating reflector on the South Shetland margin, Antarctic Peninsula. Antarctic Science, v. 5(2), p. 207- 210.

McKay, R.M., L. De Santis, D.K. Kulhanek, J.L. Ash, F. Beny, I.M. Browne, G. Cortese, I.M. Cordeiro de Sousa, J.P. Dodd, O.M. Esper, J.A. Gales, D.M. Harwood, S. Ishino, B.A. Keisling, S. Kim, S. Kim, J.S. Laberg, R.M. Leckie, J. Müller, M.O. Patterson, B.W. Romans, O.E. Romero, F. Sangiorgi, O. Seki, A.E. Shevenell, S.M. Singh, S.T. Sugisaki, T. van de Flierdt, T.E. van Peer, W. Xiao, and Z. Xiong, 2019, Expedition 374 summary. In McKay, R.M., L. De Santis, D.K. Kulhanek, and the Expedition 374 Scientists, Ross Sea West Antarctic Ice Sheet His-tory. Proceedings of the International Ocean Discovery Program, 374: College Station, TX (International Ocean Discovery Program). https://doi.org/10.14379/iodp.proc.374.101.2019

McIver, R. D., 1975, Hydrocarbon gases in canned core samples from Leg 28 sites 271, 272, and 273, Ross Sea. In: Initials reports of the Deep Sea Drilling Project, v. 28, edited by D. E. Hayes, L. A. Frakes et al., pp. 815-817, Washington, DC (US Government Printing Office), doi:10.2973/dsdp.proc.28.128.1975.

Pecher I. A., Ranero C. R., von Huene R., Minshull T. A, Singh S. C., 1998, The nature and distribution of bottom simulating reflectors at the Costa Rican convergent margin. Geophysical Journal International, 133, 219-229.

Rapp, J. B., K. A. Kvenvolden, and M. Golan-Bac, 1987, Hydrocarbon geochemistry of sediments offshore from Antarctica. In: The Antarctic Continental Margin: Geology and Geophysics of the Western Ross Sea, CPCEMR, Earth Science Series, v. 5B, edited by A. K. Cooper and F. J. Davey, p. 217-224, Huston, Texas.

Rowe M. M. and Gettrust J. F., 1993, Faulted structure of the bottom simulating reflector on the Blake Ridge, western North-Atlantic. Geology, 21, 833-836.

Ryan, W.B.F., S.M. Carbotte, J.O. Coplan, S. O'Hara, A. Melkonian, R. Arko, et al., 2009. Global Multi-Resolution Topography synthesis. Geochemistry, Geophysics, Geosystems, 10, Q03014, doi:10.1029/2008GC002332.

Sauli C., Sorlien C., Busetti M., De Santis L., Geletti R., Wardell N., Luyendyk B.P, Neogene development of Terror Rift, western Ross Sea, Antarctica. Geochemistry, Geophysics, Geosystem, accepted and resubmitted.

Sloan, E. D., 1990, Clathrate hydrates of natural gases, 1st ed., Marcel Dekker, Inc., New York and Basel, pp. 641.

Taner, M. T., F. Koehler, and R. E. Sheriff, 1979, Complex seismic trace analysis. Geophysics, v. 44(6), p. 1041-1063.

Taner, M. T., and R. E. Sheriff, 1977, Application of amplitude, frequency and other attributes to stratigraphy and hydrocarbon exploration. In: Seismic Stratigraphy: Applications to Hydrocarbon Exploration, AAPG Memoir 26, edited by C.E. Payton, Tulsa, American Association of Petroleum Geologists, p. 301-327.

Taylor, M. H., W. P. Dillon, and I. A. Pecher, 2000, Trapping and migration of methane associated with the gas hydrate stability zone at the Blake Ridge Diapir: new insights from seismic data. Marine Geology, v. 164(1/2), p. 79–89.

Vanneste, M., J. Mienert, S. Guidard, and HYDRATECH-INGGAS partners, 2002, "Arctic" gas hydrates offshore Western Svalbard, Norway. In: Proceedings of the 4th International Conference on Gas Hydrates, Yokohama, Japan, 19-23 May 2002, p. 222-227.

Vanneste, M., J. Poort, M. De Batist, and J. Klerkx, 2003, Atypical heat-flow near gas hydrate irregularities and cold seeps in the Baikal Rift Zone. Marine and Petroleum Geology, v. 19(10), p. 1257-1274.